Available online at www.sciencedirect.com
ScienceDirect
Chaos, Solitons and Fractals 38 (2008) 993–1003
CHAOS SOLITONS & FRACTALS
www.elsevier.com/locate/chaos

On the 3-dimensional k-Fibonacci spirals

Sergio Falcón *, Ángel Plaza

Department of Mathematics, University of Las Palmas de Gran Canaria (ULPGC), 35017-Las Palmas de Gran Canaria, Spain

Accepted 23 February 2007

Abstract

The 3-dimensional k-Fibonacci spirals are studied from a geometric point of view. These curves appear naturally from studying the k-Fibonacci numbers $\{F_{k,n}\}_{n=0}^{\infty}$ and the related hyperbolic k-Fibonacci functions. In this paper, after a summary of the main properties for the k-Fibonacci numbers, we focus on the geometry features (curvature and torsion) of the 3-dimensional k-Fibonacci spirals. Finally, the Metallic Shofars and their projections on the coordinate planes are also given.

1. Introduction

One of the most celebrated and ubiquitous integer sequences is the Fibonacci sequence. The Fibonacci sequence is $\{F_n\} = \{0, 1, 1, 2, 3, 5, \ldots\}$ wherein each term is the sum of the two preceding terms, beginning with the values $F_0 = 0$, and $F_1 = 1$. Particularly, Fibonacci numbers and the related Golden Mean, or Golden Section, $\phi = \frac{1+\sqrt{5}}{2}$, appear very often in theoretical physics [1–7] and physics of the high energy particles [8–11].

When we were studying some geometric properties of the well-known four-triangle longest-edge (4TLE) partition [12], we found two complex valued functions $f_R(z) = \frac{1}{-z+2}$ and $f_L(z) = \frac{1}{z+1}$ which naturally inspired us to define a generalization of the classical Fibonacci sequence [13,14] in Definition 1.

The associated matrices to functions f_R and f_L are, respectively $R = \begin{pmatrix} 0 & 1 \\ -1 & 2 \end{pmatrix}$, and $L = \begin{pmatrix} 0 & 1 \\ 1 & 1 \end{pmatrix}$. The composition of two of such functions has as associated matrix the product of the matrices associated to the two initial transformations, and, hence, any particular combination of transformations f_R and f_L is determined by the product of the corresponding matrices in the same order.

Let us find the product $R^{k-1}L$ associated to the composition $f_R^{k-1} \circ f_L$ which will be used bellow. It is easy to prove that

$$R^{k-1} = \begin{pmatrix} -k+2 & k-1 \\ -k+1 & k \end{pmatrix} \quad \text{for} \quad k \geqslant 1$$

and so

* Corresponding author. Tel.: +34 928 45 88 27; fax: +34 928 45 87 11.
E-mail address: sfalcon@dma.ulpgc.es (S. Falcón).

0960-0779/$ - see front matter © 2007 Elsevier Ltd. All rights reserved.
doi:10.1016/j.chaos.2007.02.009

$$R^{k-1}\cdot L=\begin{pmatrix}-k+2 & k-1\\ -k+1 & k\end{pmatrix}\cdot\begin{pmatrix}0 & 1\\ 1 & 1\end{pmatrix}=\begin{pmatrix}k-1 & 1\\ k & 1\end{pmatrix}$$

Definition 1. For any integer number $k\geqslant 1$, the k-Fibonacci sequence, say $\{F_{k,n}\}_{n\in\mathbf{N}}$ is defined recurrently by:

$$F_{k,0}=0, F_{k,1}=1,\quad \text{and}\quad F_{k,n+1}=kF_{k,n}+F_{k,n-1}\quad \text{for}\quad n\geqslant 1$$

Particular cases of the previous definition are:

- If $k=1$, the classical Fibonacci sequence is obtained:
  $F_0=0, F_1=1$, and $F_{n+1}=F_n+F_{n-1}$ for $n\geqslant 1$:
  $\{F_n\}_{n\in\mathbf{N}}=\{0,1,1,2,3,5,8,\ldots\}$
- If $k=2$, the Pell sequence appears:
  $P_0=0, P_1=1$, and $P_{n+1}=2P_n+P_{n-1}$ for $n\geqslant 1$:
  $\{P_n\}_{n\in\mathbf{N}}=\{0,1,2,5,12,29,70,\ldots\}$

The relation between matrix $(R^{k-1}\cdot L)$ and the k-Fibonacci sequence is given by the following proposition.

Proposition 2. *For any integer $n\geqslant 1$ holds*:

$$(R^{k-1}\cdot L)^n=\begin{pmatrix}F_{k,n+1}-F_{k,n} & F_{k,n}\\ F_{k,n+1}-F_{k,n-1} & F_{k,n}+F_{k,n-1}\end{pmatrix}$$

In [14], the following properties are proven.

Proposition 3. (*Sum of the first n k-Fibonacci numbers*)

$$\sum_{i=0}^{n}F_{k,i}=\frac{1}{k}(F_{k,n+1}+F_{k,n}-1)$$

- Sum of the first n even k-Fibonacci numbers: $\sum_{i=0}^{n}F_{k,2i}=\frac{1}{k}(F_{k,2n+1}-1)$
- Sum of the first n odd k-Fibonacci numbers: $\sum_{i=0}^{n}F_{k,2i+1}=\frac{1}{k}F_{k,2n+2}$
- Sum of the first n k-Fibonacci numbers of order $4i+1$: $\sum_{i=0}^{n}F_{k,4i+1}=\frac{1}{k}F_{k,2n+1}F_{k,2n+2}$

Proposition 4 (Livio's formula [15]). *For each not-vanishing real number p*:

$$\sum_{j=0}^{n}\frac{F_{k,j}}{p^j}=\frac{-p}{p^2-kp-1}\left[\frac{1}{p^{n+1}}(pF_{k,n+1}+F_{k,n})-1\right]$$

- For each real number p, such that $p>\frac{k+\sqrt{k^2+4}}{2}$ and by taking limits in Livio's formula: $\lim_{n\to\infty}\sum_{j=0}^{n}\frac{F_{k,j}}{p^j}=\frac{p}{p^2-kp-1}$, and $f(x)=\frac{x}{x^2-kx-1}$ is the generating function of the k-Fibonacci sequence $\{F_{k,n}\}=\{0,1=F_{k,1},F_{k,2},\ldots\}$.

Proposition 5 (*Convolution product*).

$$F_{k,n+m}=F_{k,n+1}F_{k,m}+F_{k,n}F_{k,m-1}$$

- If $k=1$, for the classical Fibonacci sequence is obtained: $F_{n+m}=F_{n+1}F_m+F_nF_{m-1}$ (Honsberger's formula [15]).
- Even terms (if $m=n$):

$$F_{k,2n}=\frac{1}{k}(F_{k,n+1}^2-F_{k,n-1}^2)$$

- Odd terms (if $m=n+1$):

$$F_{k,2n+1}=F_{k,n+1}^2+F_{k,n}^2$$

- Multiple of 3 terms (if $m=2n$):

$$F_{k,3n}=\frac{1}{k}(F_{k,n+1}^3+kF_{k,n}^3-F_{k,n-1}^3)$$

- Multiple of 4 terms (if $m = 3n$):

$$F_{k,4n} = \frac{1}{k}(F_{k,n+1}^4 + 2k^2F_{k,n}^4 - F_{k,n-1}^4) + 4F_{k,n}^3F_{k,n-1}$$

In [16,17], other approaches to the k-Fibonacci numbers have been presented. They are summarized in the sequel.

Proposition 6. (*Binet's formula*) *The n-th k-Fibonacci number is given by*:

$$F_{k,n} = \frac{r_1^n - r_2^n}{r_1 - r_2}$$

where r_1, r_2 are the roots of the characteristic equation $r^2 - kr - 1 = 0$.

Proposition 7. (*A second formula for obtaining the general term of the k-Fibonacci numbers*)

$$F_{k,n} = \frac{1}{2^{n-1}} \sum_{i=0}^{\left\lfloor \frac{n-1}{2} \right\rfloor} \binom{n}{2i+1} k^{n-1-2i}(k^2+4)^i$$

where $\lfloor a \rfloor$ *is the floor function of a, that is* $\lfloor a \rfloor = \sup\{n \in N | n \leqslant a\}$ *and says the integer part of a, for* $a \geqslant 0$.

Proposition 8. (*Limit of the quotient of two consecutive terms*)

$$\lim_{n\to\infty} \frac{F_{k,n}}{F_{k,n-1}} = \sigma_k,$$

where $\sigma_k = \frac{k+\sqrt{k^2+4}}{2}$ *is known as k-th metallic ratio.*

Proposition 9. (*A third formula for obtaining the general term of the k-Fibonacci sequence*)

$$F_{k,n} = \sum_{i=0}^{\left\lfloor \frac{n-1}{2} \right\rfloor} \binom{n-1-i}{i} k^{n-1-2i}, \quad \text{for} \quad n \geqslant 1$$

Proposition 10. (*Catalan's identity*)

$$F_{k,n-r}F_{k,n+r} - F_{k,n}^2 = (-1)^{n+1-r}F_{k,r}^2$$

Proposition 11. (*Cassini's or Simson's identity*) (*see* [18] *for the classical Fibonacci*)

$$F_{k,n-1}F_{k,n+1} - F_{k,n}^2 = (-1)^n$$

Proposition 12. (*d'Ocagne's identity*) *If* $m > n$, *then*:

$$F_{k,m}F_{k,n+1} - F_{k,m+1}F_{k,n} = (-1)^nF_{k,m-n}$$

On the other hand, in [16] both the hyperbolic k-Fibonacci sine and cosine have been defined as:

$$sF_kh(x) = \frac{\sigma_k^x - \sigma_k^{-x}}{\sigma_k + \sigma_k^{-1}}$$
$$cF_kh(x) = \frac{\sigma_k^x + \sigma_k^{-x}}{\sigma_k + \sigma_k^{-1}}$$

where σ_k is the positive root of the characteristic equation of the k-Fibonacci sequence with $\sigma_k + \sigma_k^{-1} = \sqrt{k^2+4}$. These functions are related with the classical hyperbolic sine and cosine by the following identities:

$$sF_kh(x) = \frac{2}{\sigma_k + \sigma_k^{-1}} \sinh(x \ln \sigma_k)$$
$$cF_kh(x) = \frac{2}{\sigma_k + \sigma_k^{-1}} \cosh(x \ln \sigma_k)$$

and they verify analogous properties and identities that the k-Fibonacci numbers. We refer the reader to [16] for these identities and their proofs. Also the quasi-sine k-Fibonacci function is defined as follows.

Definition 13. [16,19] The quasi-sine k-Fibonacci function is defined by

$$\mathrm{FF}_k(x) = \frac{\sigma^x - \cos(\pi x)\sigma^{-x}}{\sigma + \sigma^{-1}}$$

where σ is the positive characteristic root.

Notice that $\mathrm{FF}_k(n) = F_{k,n}$ for all integer n.

There are several identities for these quasi-sine k-Fibonacci functions which are versions of analogous identities of the k-Fibonacci numbers [17]. For example, Catalan's identity, Simson's identity, asymptotic quotient, etc.

Finally, in [17] the 3-dimensional k-Fibonacci spiral is introduced as follows.

Definition 14. The following complex valued function is called the 3-dimensional k-Fibonacci spiral:

$$\mathrm{CFF}_k(x) = \frac{\sigma^x - \cos(\pi x)\sigma^{-x}}{\sigma + \sigma^{-1}} + \mathrm{i}\frac{\sin(\pi x)\sigma^{-x}}{\sigma + \sigma^{-1}}.$$

Function $\mathrm{CFF}_k(x)$ can be written also as $\mathrm{CFF}_k(x) = \frac{\sigma^x + \mathrm{i}e^{\mathrm{i}\pi\left(\frac{1}{2}-x\right)}\sigma^{-x}}{\sigma+\sigma^{-1}}$.

It should be noted that, like the k-Fibonacci hyperbolic functions and also the quasi-sine k-Fibonacci functions, these 3-dimensional k-Fibonacci spirals verify many properties and identities as the k-Fibonacci numbers, but these relations are not the focus of our present work.

Instead we are interested here in a geometrical study of the following 3-dimensional curves of parametric equations:

$$\left\{\begin{array}{l} x = t \\ y = \frac{\sigma^t - \cos(\pi t)\sigma^{-t}}{\sigma+\sigma^{-1}} \\ z = \frac{\sin(\pi t)\sigma^{-t}}{\sigma+\sigma^{-1}} \end{array}\right\}$$

Notice that in this equation $y = \mathrm{Re}(\mathrm{CFF}_k(t))$ while $z = \mathrm{Im}(\mathrm{CFF}_k(t))$, and therefore, these curves will also be called 3-dimensional k-Fibonacci spirals.

2. Geometric study of the 3-dimensional k-Fibonacci spirals

2.1. Curvature and torsion and of some basic spirals

Let C be a curve into the 3-dimensional Euclidean space. C may be defined by its position vector $\vec{r}(t) = (x(t), y(t), z(t))$. As it is well-known the curvature of curve C is defined by the formula $\kappa = \frac{|\vec{r}' \wedge \vec{r}''|}{|\vec{r}'|^3}$, where $|\vec{r}' \wedge \vec{r}''|$ is for the module of the cross-product. Therefore, an arc of a curve is said to be of null curvature if its points are in the same straight line. In other case, the curvature is not null.

Torsion is defined by the expression $\tau = \frac{[\vec{r}', \vec{r}'', \vec{r}''']}{|\vec{r}' \wedge \vec{r}''|^2}$, where $[\vec{r}', \vec{r}'', \vec{r}''']$ indicates the scalar triple product. It is said that a curve arc is of zero torsion if their point are on the same plane. For a given curve, the torsion indicates how far away the curve is from a plane.

In this section, we focus on the curvature and the torsion of the 3-dimensional k-Fibonacci spirals. Before to tackle this issue, let us recall the easiest examples of spirals.

The simplest 3-dimensional spiral is a circular or cylindric spiral, also known as circular helix. A circular helix is a curve for which the tangent makes a constant angle with a fixed line. The shortest path between two points on a cylinder (one not directly above the other) is a fractional turn of a circular helix, as it can be seen by cutting the cylinder along one of its sides, flattening it out. The double helix shape is commonly associated with DNA, since the double helix is the structure of DNA. This fact was published for the first time by James D. Watson and Francis Crick in 1953 [20]. They constructed a molecular model of DNA in which there were two complementary, antiparallel (side-by-side in opposite directions) strands of the bases guanine, adenine, thymine, and cytosine, covalently linked through phosphodiester bonds. Each strand forms a helix, and the two helices are held together through hydrogen bonds, ionic forces, hydrophobic interactions, and van der Waals forces forming a double helix.

The circular helix is a 3-dimensional curve with parametric equations:

$$\left\{\begin{array}{l} x = r\cos t \\ y = r\sin t \\ z = pt \end{array}\right\}$$

in which t represents the intersection angle with the generation axis, r is the radius of the cylinder and $2p\pi$ is a constant giving the vertical separation of the helix's loops, also known as thread. See Fig. 1.

By applying the preceding formulas, we can find that the curvature of the helix is given by $\kappa = \frac{r}{r^2+p^2}$, while the torsion is $\tau = \frac{p}{r^2+p^2}$, and therefore $\frac{\kappa}{\tau} = \frac{r}{p}$, which is a constant. In fact, Lancret's theorem states that a curve is a helix if and only if the ratio of curvature to torsion is constant [21,22].

Let us go now to a spatial curve more complicated than the circular helix and for which both curvature and torsion are not constant. A conical spiral is the spacial curve cutting the generatrices of a right cone at constant angle. Its parametric equations are:

$$\left\{\begin{array}{l} x = rt\cos t \\ y = rt\sin t \\ z = pt \end{array}\right\}$$

where t is the angle of rotation.

For $r = p = 1$ the curvature of the conical spiral is variable and equal to $\kappa(t) = \sqrt{\frac{t^4+5t^2+8}{(t^2+2)^3}}$. For values of parameter t between -5 and 5, the points of coordinates $(t, \kappa(t))$ follow a curve similar to the Agnesi curve, achieving its maximum value at $t = 0$. See Fig. 2a.

The torsion of this conical spiral is given by the formula $\tau(t) = \frac{t^2+6}{t^4+5t^2+8}$, which presents a similar shape that the curvature, but with a maximum value of $\frac{3}{4}$ at $t = 0$. See Fig. 2b. In any case, it should be noted that both the curvature and the torsion of a conical spiral presents a smooth behavior for all values in $(-\infty, +\infty)$.

From now on, we focus on the 3-dimensional k-Fibonacci spirals. We shall show that the behavior of both curvature and torsion is much more complex than the cylindrical or conical spirals. In the 3-dimensional k-Fibonacci spirals the curvature as well as the torsion are continuous functions not only of argument x but also of parameter k.

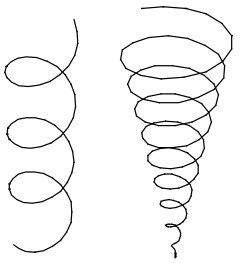

Fig. 1. Circular spiral or circular helix (left) and a conical spiral (right).

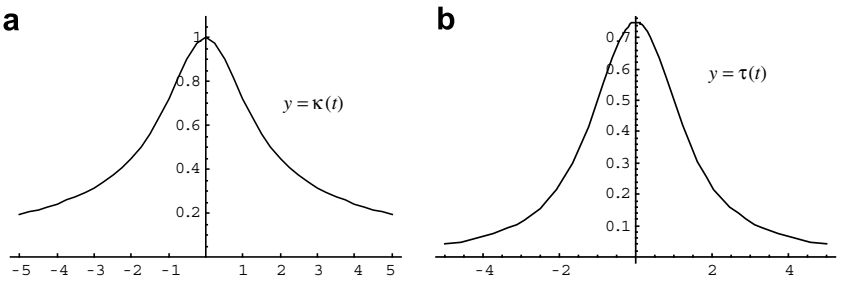

Fig. 2. Curvature function and torsion function for a conical spiral with $r = k = 1$.

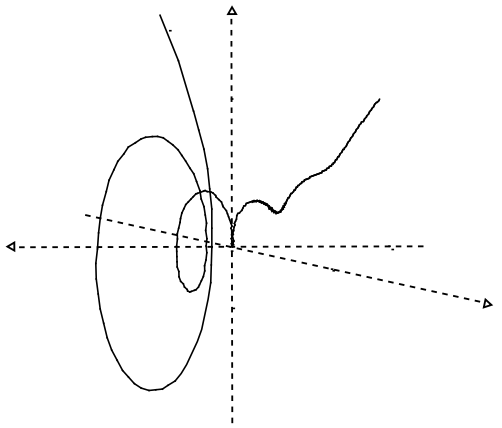

Fig. 3. The 3-dimensional k-Fibonacci spiral, for $k = 1$.

2.2. Curvature of the 3-dimensional k-Fibonacci spiral

Let us consider the 3-dimensional k-Fibonacci spiral with vector equation:

$$\vec{r} = \left(x, \frac{\sigma^x - \cos(\pi x)\sigma^{-x}}{\sigma + \sigma^{-1}}, \frac{\sin(\pi x)\sigma^{-x}}{\sigma + \sigma^{-1}}\right)$$

where $\sigma = \frac{k+\sqrt{k^2+4}}{2}$. See [19]. The graphics of these spirals are of the same shape, and therefore, we show the 3-dimensional 1-Fibonacci spiral in Fig. 3.

By using MATHEMATICA © the curvature can be calculated, since $\kappa(x,k) = \frac{A(x,k)}{B(x,k)}$, where

$$A(x,k) = \frac{1}{r^2\sigma^{2x}}\left(\begin{array}{l} r^2\sigma^{2x}(2\pi\cos(\pi x)\ln\sigma + (\pi^2 - \ln^2\sigma)\sin(\pi x))^2 + \\ +r^2\sigma^{2x}(\cos(\pi x)(\pi^2 - \ln^2\sigma) + \ln\sigma(\sigma^{2x}\ln\sigma - 2\pi\sin(\pi x)))^2 + \\ +(\pi(\pi^2 + \ln^2\sigma) + \sigma^{2x}\ln\sigma(3\pi\cos(\pi x)\ln\sigma + \pi^2 - 2\ln^2\sigma)\sin(\pi x)) \end{array}\right)^{\frac{1}{2}}$$

$$B(x,k) = \frac{(r^2 + \sigma^{2x}\ln^2\sigma + \sigma^{-2x}(\pi^2 + \ln^2\sigma) + 2\ln\sigma(\cos(\pi x)\ln\sigma + \pi\sin(\pi x)))^{\frac{3}{2}}}{r^3}$$

and the graphics of these functions for several values of parameter k are shown in Fig. 4. After studying the curvature function for many values of k it can be said these functions present a unique maximum for $x < 0$ close to the origin, while for $x > 0$ they show another maximum. Table 1 gives the maximum values and the point in which these maximum are obtained. The absolute maximum for $y = \kappa(x,k)$ is achieved for $k = 1$ at $x = 1.475$ meanwhile for any other integer value of k the maximum is presented at negative values of x.

The general behavior of the torsion function for the 3-dimensional k-Fibonacci spirals is quite similar for different values of $k \in N$, with the exception of the case $k = 1$, as we will show bellow.

2.3. Torsion of the 3-dimensional k-Fibonacci spiral

Torsion of the 3-dimensional k-Fibonacci spiral is given by $\tau(x,k) = \frac{C(x,k)}{D(x,k)}$, where

$$C(x,k) = 2r^2\sigma^{2x}(-\pi(\pi^2 + t^2)^2 - \sigma^{2x}t^2(\pi\cos(\pi x)(\pi^2 - 5t^2) + 2t(-\pi^2 + t^2)\sin(\pi x)))$$

$$\begin{aligned} D(x,k) = {} & 2r^2\sigma^{6x}t^4 + 2\pi^2(\pi^2 + t^2)^2 + 2\sigma^{2x}(\pi^2 + t^2) \\ & \times [r^2(\pi^2 + t^2) + 2\pi t[3\pi\cos(\pi x)t + (\pi^2 - 2t^2)\sin(\pi x)]] - \sigma^{4x}t^2 \\ & \times \left[\begin{array}{l} 4r^2\cos(\pi x)(-\pi^2 + t^2) - (\pi^2 + t^2)(\pi^2 + 4t^2) + \cos(2\pi x) \\ \times(\pi^4 - 13\pi^2t^2 + 4t^4) + 2\pi t[4r^2\sin(\pi x) - 3(\pi^2 - 2t^2)\sin(2\pi x)] \end{array}\right] \end{aligned}$$

where $t = \ln\sigma$. Again, by using MATHEMATICA © we draw the torsion functions for different values of parameter k and the graphics are shown in Fig. 5.

Torsion curve does not present any relative maximum for $x < 0$, but, in exchange there are an infinite number of maximum for positive x, as Table 2 shows. It should be noted that Table 2 only shows the closest maximum to the

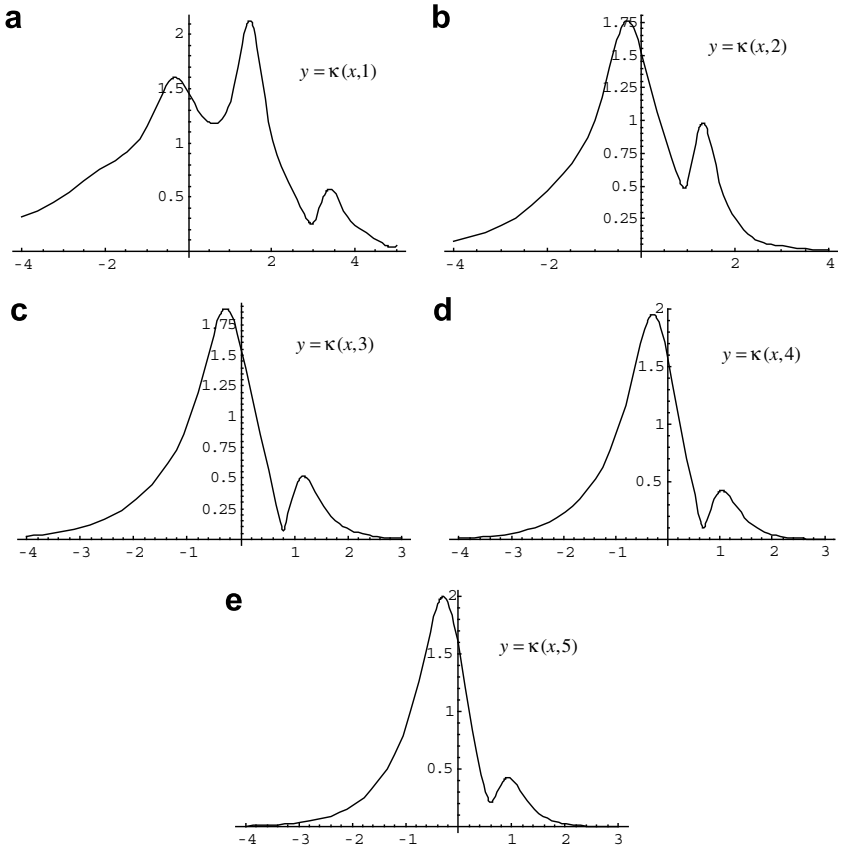

Fig. 4. Curvature functions $y = \kappa(x,k)$ for $k = 1$–5.

Table 1
Maximum values of curvature $y = \kappa(x,k)$ for different values of k

k	$(x < 0, \max)$	$(x > 0, \max)$
1	$(-0.325, 1.6028)$	$(1.475, 2.1278)$
2	$(-0.290, 1.7637)$	$(1.320, 0.9808)$
3	$(-0.280, 1.8805)$	$(1.170, 0.5146)$
4	$(-0.285, 1.9540)$	$(1.040, 0.4239)$
5	$(-0.290, 1.9966)$	$(0.930, 0.4259)$
6	$(-0.300, 2.0196)$	$(0.84, 0.4600)$
7	$(-0.315, 2.0311)$	$(0.775, 0.5068)$
8	$(-0.325, 2.0361)$	$(0.725, 0.5582)$
9	$(-0.340, 2.0377)$	$(0.690, 0.6100)$
10	$(-0.350, 2.0377)$	$(0.665, 0.6603)$
15	$(-0.410, 2.0382)$	$(0.600, 0.8719)$
20	$(-0.445, 2.0506)$	$(0.575, 1.0255)$
25	$(-0.470, 2.0700)$	$(0.57, 1.1410)$
100	$(-0.580, 2.3455)$	$(0.600, 1.7609)$

origin, but, there are infinite maximums for x bigger enough. For instance, for $k = 1$ there is a maximum at $x = 130.71$, with value 3.17×10^{-53}, while for $k = 3$ there is another maximum at $x = 130.35$ with value 1.315×10^{-134}, and finally, for example, for $k = 5$ there is a maximum at $x = 100.18$ with value 6.8×10^{-143}.

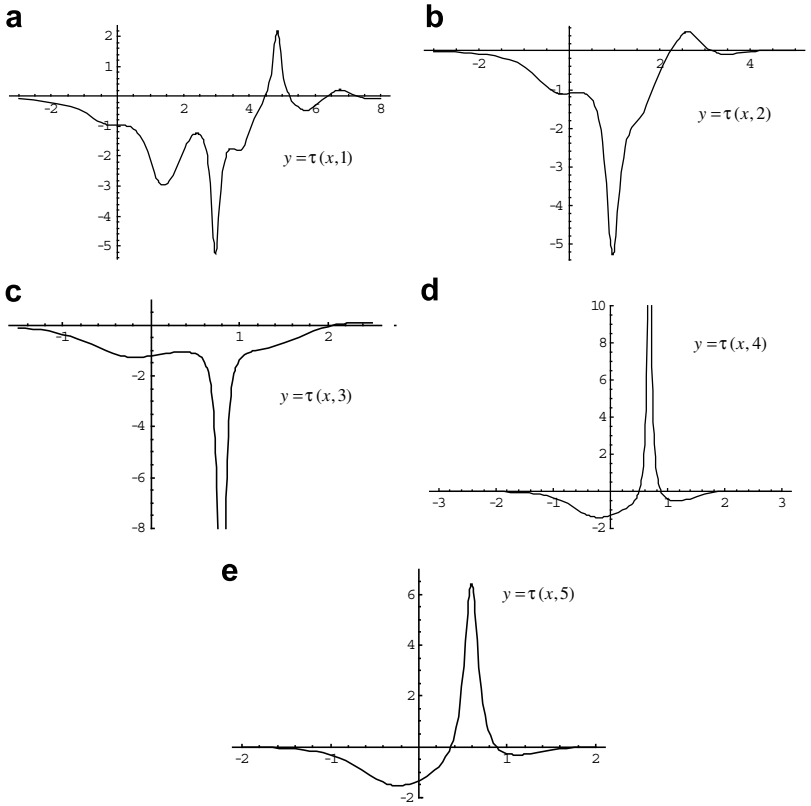

Fig. 5. Torsion functions $\tau(x,k)$ for $k = 1$–5.

Table 2
Maximum values of torsion $y = \tau(x,k)$ for different values of k

k					
1	$(0.1,-0.969)$	$(2.42,-1.237)$	$(3.47,-1.740)$	$(4.85,2.208)$	$(6.76,0.22)$
2	$(0.21,-1.077)$	$(2.62,0.505)$	$(4.51,0.015)$	$(6.5,0.0005)$	$(8.5,10^{-5})$
3	$(0.37,-1.062)$	$(2.38,0.087)$	$(4.35,0.0007)$	$(6.35,6\times10^{-6})$	$(8.4,5\times10^{-8})$
4	$(0.68,13.507)$	$(2.26,0.027)$	$(4.25,8\times10^{-5})$	$6.25,2.6\times10^{-5})$	$\cdots$
5	$(0.6,6.373)$	$(2.18,0.011)$	$(4.18,1.5\times10^{-5})$	$\cdots$	

Some remarks are in order for the case k integer:

- Torsion curves $\tau(x,k)$ show an infinite number of maximum for $x > 0$.
- If $k = 1$, the first three maximum values are negative and less than the preceding one, while for $k = 2$ and $k = 3$ only the first maximum is negative, and the rest of them are positive.
- For $k > 3$ all the maximums are positive.

3. The Metallic Shofars

Real and imaginary parts of the 3-dimensional k-Fibonacci spiral are, respectively, $\mathrm{Re}(\mathrm{CFF}_k(x)) = \frac{\sigma^x - \cos(\pi x)\sigma^{-x}}{\sigma+\sigma^{-1}} = y(x)$, $\mathrm{Im}(\mathrm{CFF}_k(x)) = \frac{\sin(\pi x)\sigma^{-x}}{\sigma+\sigma^{-1}} = z(x)$. By considering $\mathrm{Re}(\mathrm{CFF}_k(x))$ as function $y(x)$, and $\mathrm{Im}(\mathrm{CFF}_k(x))$ as function $z(x)$, then Y-axis can be seen as real axis, and Z-axis as imaginary axis. Therefore, we can write the following system of equations:

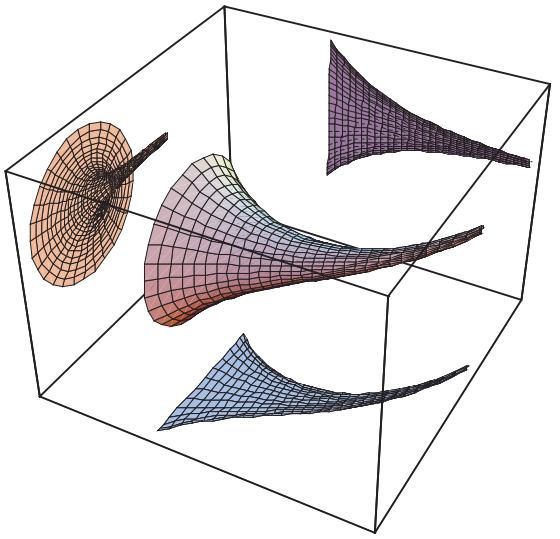

Fig. 6. The Golden Shofar and its projections on the coordinate planes.

$$\left\{\begin{array}{ccc} y(x)-\frac{\sigma^x}{\sigma+\sigma^{-1}} & = & -\frac{\cos(\pi x)\sigma^{-x}}{\sigma+\sigma^{-1}} \\ z(x) & = & \frac{\sin(\pi x)\sigma^{-x}}{\sigma+\sigma^{-1}} \end{array}\right\}$$

By summing up the squares of previous expressions and considering y and z as independent variables the following equation is obtained:

$$\left(y-\frac{\sigma^x}{\sigma+\sigma^{-1}}\right)^2+z^2=\left(\frac{\sigma^{-x}}{\sigma+\sigma^{-1}}\right)^2 \tag{1}$$

This equation corresponds to a surface which have been called Metallic Shofar [17]. The graphics of the Metallic Shofars are similar to each other. Note that in the case $k=1$ we obtain the *Golden Shofar* [23] with equation $\left(y-\frac{\tau^x}{\sqrt{5}}\right)^2+z^2=\frac{1}{5\tau^{2x}}$, where τ is the Golden Ratio. The shape of the Golden Shofar, and its projections on the coordinate planes, are shown in Fig. 6.

For the case $k=2$ the *Silver Shofar* with equation $\left(y-\frac{\varphi^x}{\sqrt{8}}\right)^2+z^2=\frac{1}{8\varphi^{2x}}$ is obtained, where $\varphi=1+\sqrt{2}$ is the Silver Ratio. Finally, for $k=3$ results the *Bronze Shofar* with equation $\left(y-\frac{\psi^x}{\sqrt{13}}\right)^2+z^2=\frac{1}{13\psi^{2x}}$, where $\psi=\frac{3+\sqrt{13}}{2}$ is the Bronze Ratio [24]. Fig. 7 shows the Metallic Shofars for $k=2$ and 3.

By construction of the Metallic Shofars it is deduced that the 3-dimensional k-Fibonacci spiral lives into the corresponding Metallic Shofar.

By doing first $z(x)=0$, then $y(x)=0$, and finally $x=0$ into Eq. (1) the projection of the Metallic Shofar on the respective coordinate plane is obtained as follows.

(a) The projection on plane XOY, $(z(x)=0)$ results into the regions limited by the curves with equations $y(x)=\frac{\sigma^x+\sigma^{-x}}{\sigma+\sigma^{-1}}$ and $y(x)=\frac{\sigma^x-\sigma^{-x}}{\sigma+\sigma^{-1}}$, which are respectively, the so-called hyperbolic k-Fibonacci sine and cosine as defined in [17]. This projection is shown in Fig. 8. The upper curve corresponds to the hyperbolic k-Fibonacci cosine, the lower curve is for the hyperbolic k-Fibonacci sine, and the interior curve is the projection of the respective 3-dimensional k-Fibonacci spiral. Also note that the symmetry axis (or medial axis) of this projected region is the exponential curve $y(x)=\frac{\sigma^x}{\sigma+\sigma^{-1}}$ and it is shown in Fig. 9.

(b) The projection on plane XOZ, $(y=0)$ results into the region limited by the exponential curves with equations $z(x)=\frac{\sigma^{-x}}{\sigma+\sigma^{-1}}$ and $z(x)=-\frac{\sigma^{-x}}{\sigma+\sigma^{-1}}$. This projection is shown in Fig. 10. The interior curve is the projection of the respective 3-dimensional k-Fibonacci spiral, and this projected curve has equation $z(x)=\frac{\sin(\pi x)\sigma^{-x}}{\sigma+\sigma^{-1}}$. Note that the symmetry axis is the Z-axis.

(c) Finally, every plane parallel to plane YOZ cuts the Metallic Shofar in a circle centered at $\left(0,\frac{\sigma^x}{\sigma+\sigma^{-1}}\right)$ and with radius $r=\frac{\sigma^x}{\sigma+\sigma^{-1}}$.

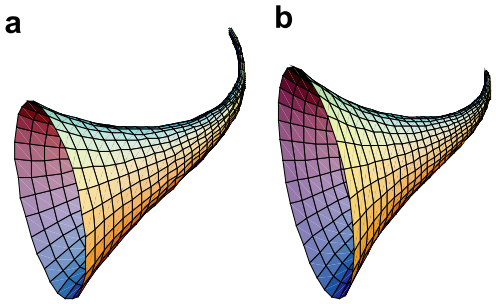

Fig. 7. The Metallic Shofars.

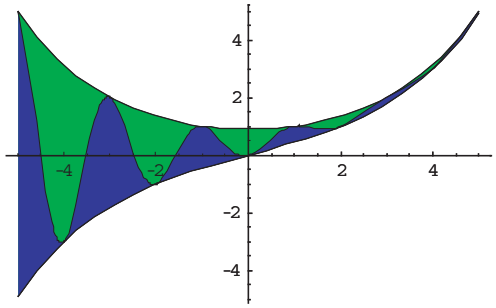

Fig. 8. Projection of a Metallic Shofar along with the corresponding 3-D Fibonacci spiral over the XOY coordinate plane.

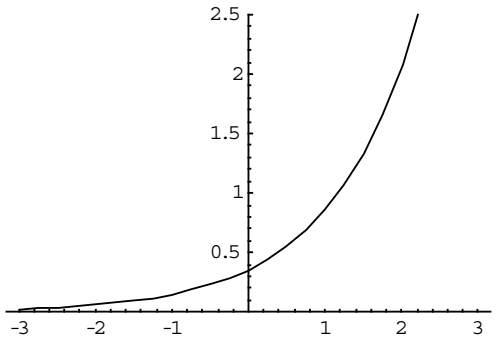

Fig. 9. Medial axis of the projection of a Metallic Shofar over the XOY coordinate plane.

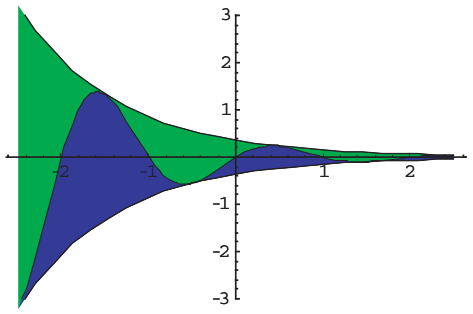

Fig. 10. Projection of a Metallic Shofar along with the corresponding 3-D Fibonacci spiral over the XOZ coordinate plane.

The relation between the 3-dimensional k-Fibonacci spiral and the hyperbolic k-Fibonacci functions sine and cosine is obtained as follows. From Eq. (1) we get

$$z^2 = \left(\frac{\sigma^{-x}}{\sigma+\sigma^{-1}}\right)^2 - \left(y - \frac{\sigma^{x}}{\sigma+\sigma^{-1}}\right)^2$$

And, therefore,

$$z^2 = \left[\frac{\sigma^{-x}}{\sigma+\sigma^{-1}} - \left(y - \frac{\sigma^{x}}{\sigma+\sigma^{-1}}\right)\right] \cdot \left[\frac{\sigma^{-x}}{\sigma+\sigma^{-1}} + \left(y - \frac{\sigma^{x}}{\sigma+\sigma^{-1}}\right)\right]$$

So, $z^2 = (cF_k h(x) - y) \cdot (y - sF_k h(x))$.

Acknowledgement

This work has been supported in part by CICYT Project number MTM2005-08441-C02-02 from Ministerio de Educación y Ciencia of Spain.

References

[1] El Naschie MS. The golden mean in quantum geometry, Knot theory and related topics. Chaos, Solitons, & Fractals 1999;10(8):1303–7.
[2] El Naschie MS. Notes on superstrings and the infinite sums of Fibonacci and Lucas numbers. Chaos, Solitons & Fractals 2001;12(10):1937–40.
[3] El Naschie MS. Non-Euclidean spacetime structure and the two-slit experiment. Chaos, Solitons & Fractals 2005;26(1):1–6.
[4] El Naschie MS. Stability analysis of the two-slit experiment with quantum particles. Chaos, Solitons & Fractals 2005;26(2):291–4.
[5] El Naschie MS. Fuzzy dodecahedron topology and E-infinity spacetime as a model for quantum physics. Chaos, Solitons & Fractals 2006;30(5):1025–33.
[6] El Naschie MS. The Fibonacci code behind super strings and P-Branes. An answer to M. Kakus fundamental question. Chaos, Solitons & Fractals 2007;31(3):537–47.
[7] El Naschie MS. Hilbert space, Poincaré dodecahedron and golden mean transfiniteness. Chaos, Solitons & Fractals 2007;31(4):787–93.
[8] El Naschie MS. Topological defects in the symmetric vacuum, anomalous positron production and the gravitational instanton. Int J Modern Phys 2004;13(4):835–49.
[9] El Naschie MS. Experimental and theoretical arguments for the number and mass of the Higgs particles. Chaos, Solitons & Fractals 2005;23:1091–8.
[10] El Naschie MS. Deriving the essential features of the standard model from the general theory of relativity. Chaos, Solitons & Fractals 2005;24:941–6.
[11] Marek-Crnjac L. Different Higgs models and the number of Higgs particles. Chaos, Solitons & Fractals 2006;27(3):275–9.
[12] Rivara MC. Algorithms for refining triangular grids suitable for adaptive and multigrid techniques. Inter J Num Meth Eng 1984;20:745–56.
[13] Plaza A, Suárez JP, Carey GF. A geometrical diagram for similarity classes in triangle subdivision. Comput Aided Geometric Design 2007;24(1):19–27.
[14] Falcón S, Plaza A. On the Fibonacci k-numbers. Chaos, Solitons & Fractals 2007;32(2):1615–24.
[15] Livio M. The Golden ratio: the story of phi, the world's most astonishing number. New York: Broadway Books; 2002.
[16] Falcón S, Plaza A. The k-Fibonacci sequence and the Pascal 2-triangle. Chaos, Solitons & Fractals 2007;33(1):38–49.
[17] Falcón S, Plaza A. The k-Fibonacci hyperbolic functions. Chaos, Solitons & Fractals 2008;38(2):409–20.
[18] Vajda S. Fibonacci and Lucas numbers, and the golden section. Theory and applications. Chichester: Ellis Horwood limited; 1989.
[19] Stakhov A, Rozin B. The continuos functions for the Fibonacci and Lucas p-numbers. Chaos, Solitons & Fractals 2006;28:1014–25.
[20] Watson JD, Crick FH. Molecular structure of Nucleic Acids. Nature 1953;171:737–8.
[21] Lancret MA. Mémorie sur les courbes à double courbature. Mém des sav étrangèrs 1806;1:182–7.
[22] Scofield PD. Curves of constant precession. The Am Math Monthly 1995;102(6):531–7.
[23] Stakhov A, Rozin B. The Golden Shofar. Chaos, Solitons & Fractals 2005;26(3):677–84.
[24] Spinadel VW. The metallic means family and forbidden symmetries. Int Math J 2002;2(3):279–88.